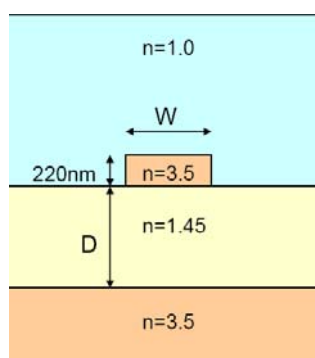


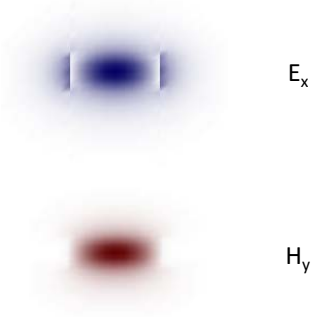
Vlnovody s velkým kontrastem indexu lomu

„Fotonický drát“

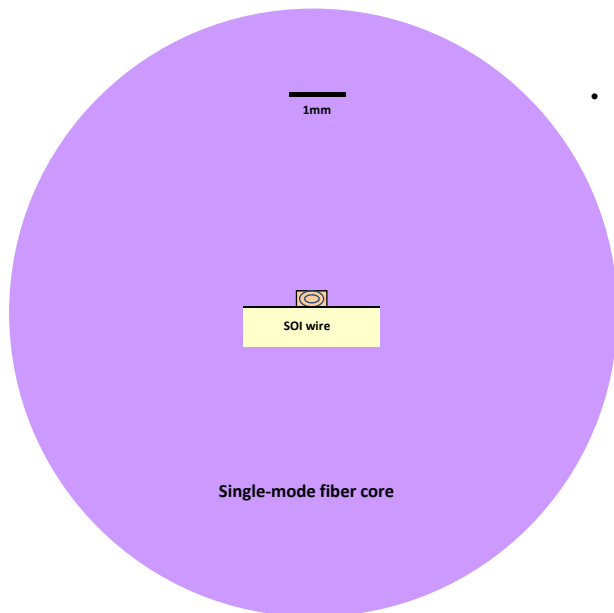
(vlnovod s velkým kontrastem indexu lomu)



Rozložení elektromagnetického pole základního vidu TE_{00}

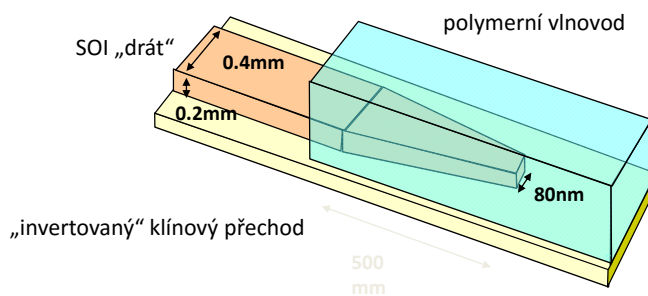
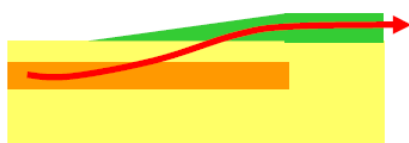


Vazba do „nanofotonických“ vlnovodů

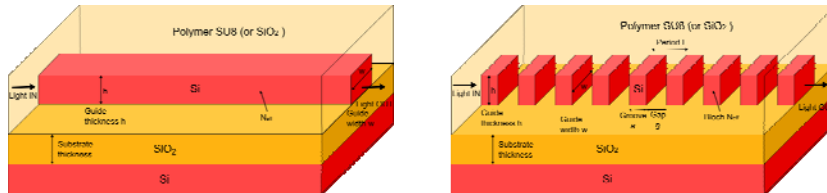


- **Problémy:**
 - Účinná vazba mezi submikrometrovým vlnovodem a vláknem
 - Je nutný konvertor velikosti vidového pole:
 - v horizontální rovině
 - ve vertikální rovině (obtížnější)
 - Polarizační problém

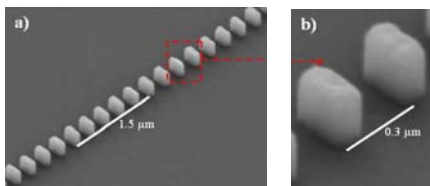
„Adiabatický přechod“ mezi vlnovody velmi různých profilů / kontrastů



Křemíkové vlnovody se subvlnovými strukturami (subwavelength grating waveguide, SWG)



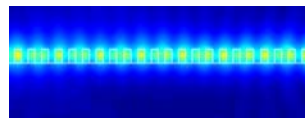
Schematic picture of (a) a strip channel waveguide and (b) SWG waveguide considered in this contribution. In both cases, Si guide (either continuous or segmented) on SiO₂ substrate, embedded in SU8 polymer (or, alternatively in SiO₂ cladding) are considered; h represents the guide thickness, w guide width, L is the SWG period (with Si groove dimension a, and gap g).



Scanning electron microscope (SEM) images of fabricated structures including: a) SWG straight waveguide with $\Lambda = 300$ nm, $w = 250$ nm and a duty cycle of 33%. b) Detail of two SWG segments.

P. J. Bock, Optics Express, 18(19), 20251 (2010).

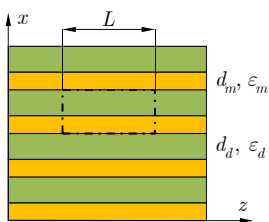
- SWG waveguide - a new type of microphotonic waveguide
- Practical implementations to fiber-chip coupling, waveguide crossing and refractive index engineering



ELEMENTÁRNÍ TEORIE EFEKTIVNÍHO PROSTŘEDÍ (Effective medium theory, EMT)

Vrstevnaté prostředí s parametry ε_1 , d_1 a ε_2 , d_2

$$d_1, d_2 \ll \lambda$$



Ekvivalentní kapacitor s deskami podél x:

$$C_{eq} = \frac{\varepsilon_1 d_1}{L} + \frac{\varepsilon_2 d_2}{L} = \frac{\varepsilon_{||} (d_1 + d_2)}{L}; \quad \varepsilon_{||} \dots \text{eff. permittivity}$$

Tedy $\varepsilon_{||} = f\varepsilon_1 + (1-f)\varepsilon_2$, $f = \frac{d_1}{d_1 + d_2} = \frac{d_1}{L}$

Ekvivalentní kapacitor s deskami podél z: $0 \leq f \leq 1$.

$$\frac{1}{C_{eq}} = \frac{d_1}{\varepsilon_1 L} + \frac{d_2}{\varepsilon_2 L} = \frac{(d_1 + d_2)}{\varepsilon_{\perp} L} \quad \varepsilon_{\perp} \dots \text{eff. permittivity},$$

Tedy $\frac{1}{\varepsilon_{\perp}} = \frac{1}{\varepsilon_1} f + \frac{1}{\varepsilon_2} (1-f)$, $\varepsilon_{\perp} = \frac{\varepsilon_1 \varepsilon_2}{f\varepsilon_2 + (1-f)\varepsilon_1}$,

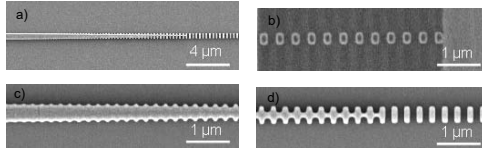
Efektivní prostředí je anizotropní, jednoosé, s tenzorem permittivity

$$\boldsymbol{\varepsilon}_{eff} = \begin{pmatrix} \varepsilon_{\perp} & 0 & 0 \\ 0 & \varepsilon_{||} & 0 \\ 0 & 0 & \varepsilon_{||} \end{pmatrix}$$

J. C. Maxwell Garnett, "Colours in metal glasses and in metallic films,"
Philosophical Transaction of the Royal Society London **203**, 385-420 (1904).

Složitější subvlnové vlnodné struktury

Vazební člen - vidový transformátor

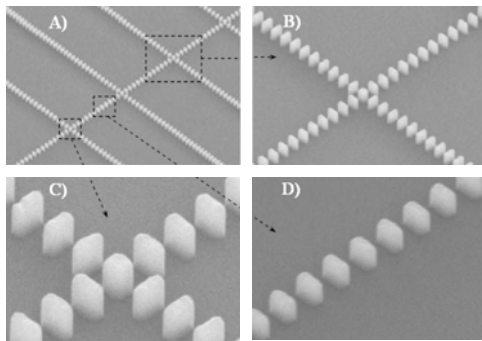


Subwavelength grating mode transformer.

- a) SEM image of the coupler,
- b) low - confinement section near the chip edge,
- c) high-confinement section near the strip waveguide,
- d) Intermediate section.

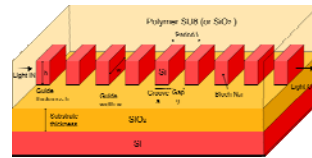
P. J. Bock et al., 7th IEEE Conference on Group IV Photonics, Sept. 2010, Beijing

Křížení segmentovaných vlnodů

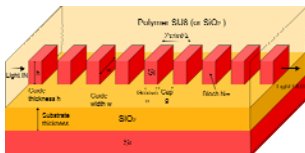


Scanning electron microscope images of SWG crossings:
 A) multiple SWG crossings,
 B) one SWG crossing,
 C) detail of the crossing region with square center segment,
 D) SWG straight waveguide.

P. J. Bock et al., Optics Express, 18(15), 16146 (2010).



DISPERSION PROPERTIES OF SWG WAVEGUIDES



Propagating modes in SWGW are **Bloch modes**

Propagation constant and the effective refractive index of the m -th Bloch mode:

$$\Gamma_{mm} = \exp(i\beta_{B,m}\Lambda), \quad \beta_{B,m} = -\frac{i}{\Lambda} \ln \Gamma_{mm} = \frac{2\pi}{\Lambda} N_{B,m}$$

Grating constant of the SWGW: $K = \frac{2\pi}{\Lambda}$

“First Brillouin zone” of the SWGW as a 1D photonic crystal: $|\beta_B| < K/2 = \pi/\Lambda$

For lossless propagation, $n_s < N_B < \frac{\lambda}{2\Lambda} = n_{BZ}$

Group effective index: $N_{B,g} = N_B - \lambda dN_B/d\lambda$

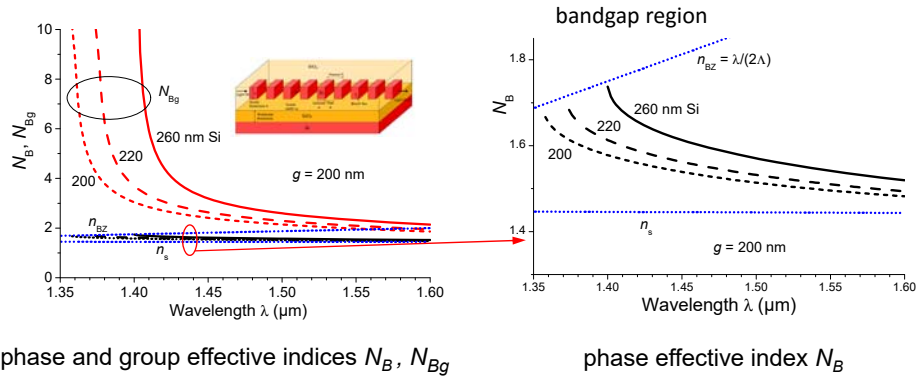
In analogy with the behaviour of photonic crystals we expect that

$$N_{B,g} \rightarrow \infty \text{ as } N_B \rightarrow \frac{\lambda}{2\Lambda} \quad (\text{the “bandgap edge”})$$

Region of N_B "close to" $\frac{\lambda}{2\Lambda}$ represents the **slow light region**

Disperzní vlastnosti SWG vlnodů

Standard SWGW, $w = 350$ nm, $\Lambda = 400$ nm, $g = 200$ nm, TE polarization

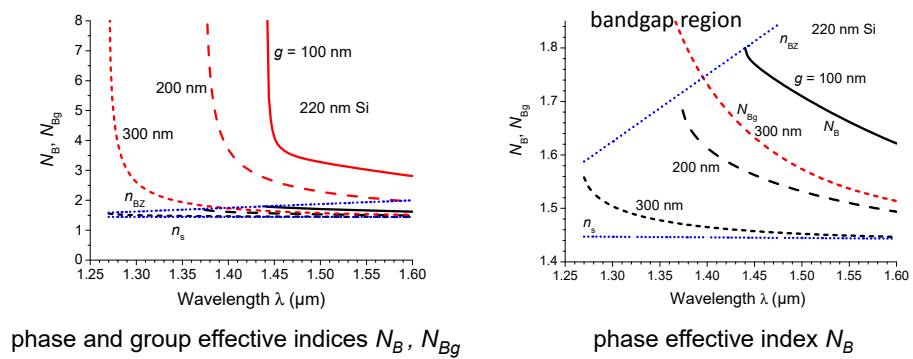


phase and group effective indices N_B, N_{Bg}

phase effective index N_B

Disperzní vlastnosti SWG vlnodů

Standard SWGW, $w = 350$ nm, $\Lambda = 400$ nm, various gap sizes g , TE polarization

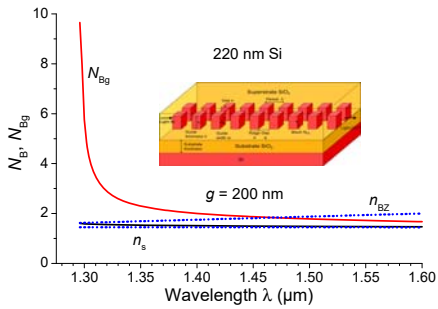


phase and group effective indices N_B, N_{Bg}

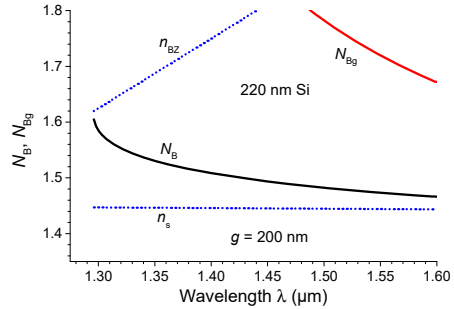
phase effective index N_B

Disperzní vlastnosti štěrbinového SWG vlnovodu

slot SWGW, width $2 \times 200 \text{ nm} + 100 \text{ nm}$ slot, $\Lambda = 400 \text{ nm}$, $g = 200 \text{ nm}$, TE polarization



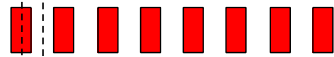
phase and group effective indices N_B, N_{Bg}



phase effective index N_B

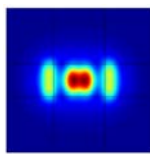
POWER DENSITY DISTRIBUTION

standard SWG waveguide

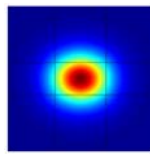


Si gap \rightarrow Bloch mode

$\lambda = 1.3 \mu\text{m}$, $g = 100 \text{ nm}$

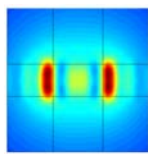


Si segment

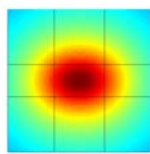


gap

$\lambda = 1.55 \mu\text{m}$, $g = 360 \text{ nm}$
(Si filling fraction = 0.1)

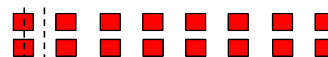


Si segment



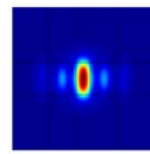
gap

slot SWG waveguide

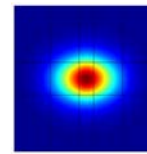


Si gap \rightarrow Bloch mode

$\lambda = 1.3 \mu\text{m}$, $g = 200 \text{ nm}$



Si segment

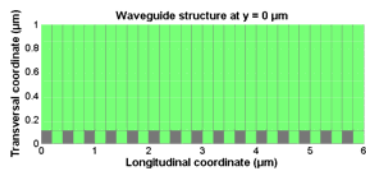
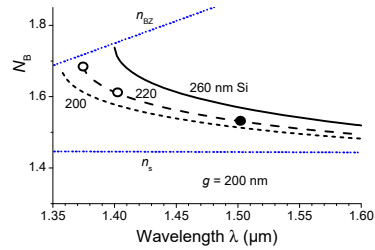
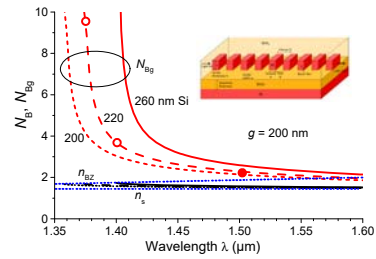


gap

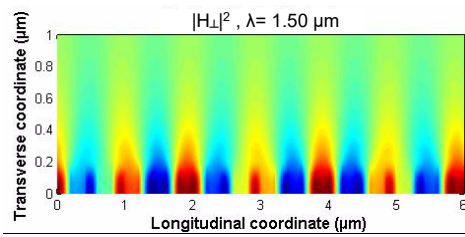
Power of the Bloch mode of the slot SWG waveguide is **very strongly** localized in a low-index medium, similarly as a mode of a uniform slot waveguide

BLOCH MODE FIELD PROPAGATION

Vertical component of the magnetic field intensity @ $\lambda = 1500$ nm

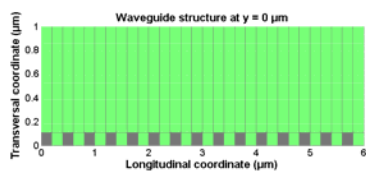
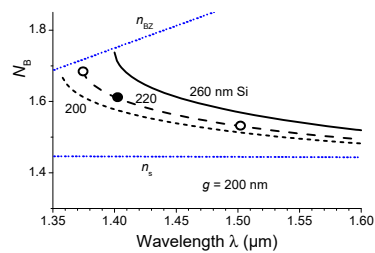
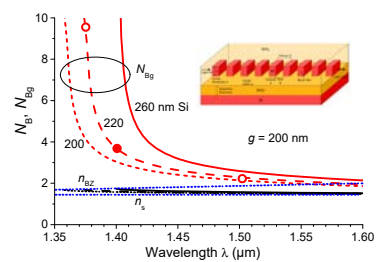


character quite similar to a uniform waveguide

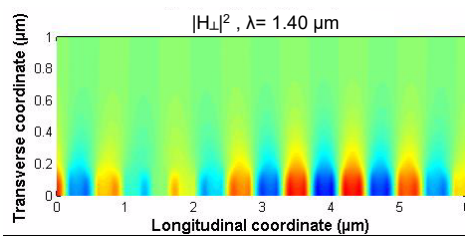


BLOCH MODE FIELD PROPAGATION

Vertical component of the magnetic field intensity @ $\lambda = 1400$ nm

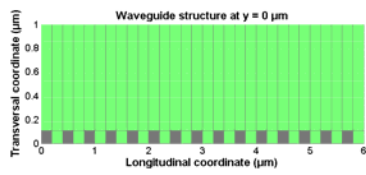
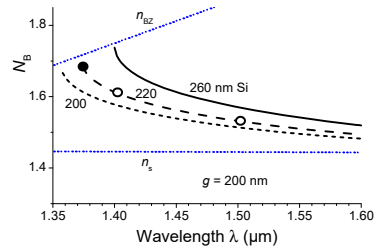
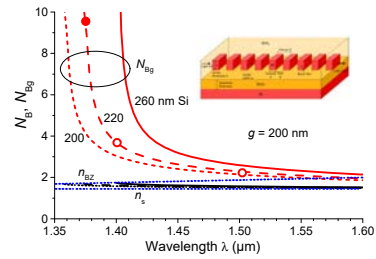


backward propagating waves are becoming important

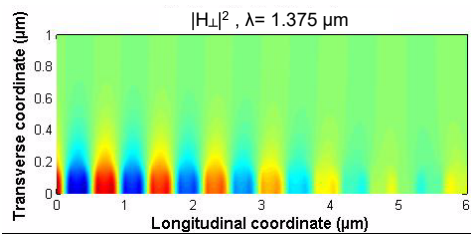


BLOCH MODE FIELD PROPAGATION

Vertical component of the magnetic field intensity @ $\lambda = 1375 \text{ nm}$

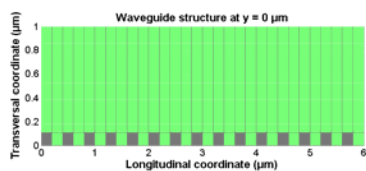
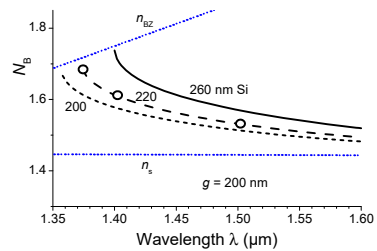
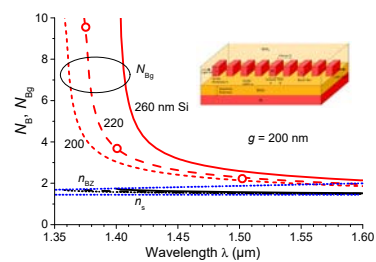


markedly resonant character

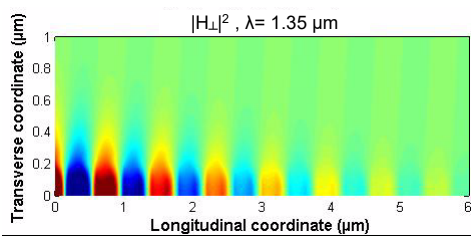


BLOCH MODE FIELD PROPAGATION

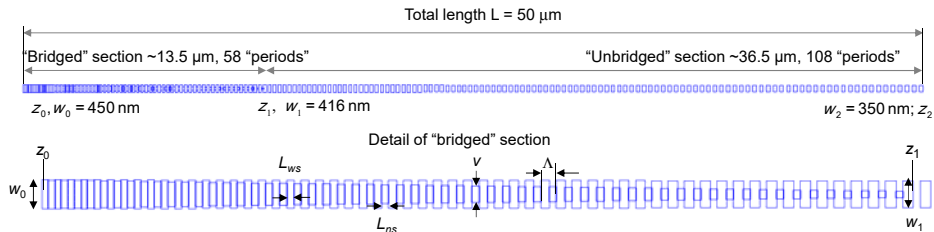
Vertical component of the magnetic field intensity @ $\lambda = 1350 \text{ nm}$



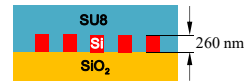
evanescent Bloch mode within the bandgap



VAZBA MEZI SWG VLNOVODEM A NANODRÁTEM



Both wide and narrow "bridged" segments are linearly tapered; the period length Λ is also linearly tapered, from 200 nm to 270 nm in the "bridged" section and from 270 nm to 400 nm in the "unbridged" section



Version 2 (L/2)

Similar (linearly tapered) but twice shorter: total length $\sim 25 \mu\text{m}$

"Bridged" section $\sim 6.75 \mu\text{m}$, 29 "periods", "unbridged" section $\sim 18.25 \mu\text{m}$, 54 "periods"

Version 3 (L/4)

Similar (linearly tapered) but four-times shorter: total length $\sim 12.5 \mu\text{m}$

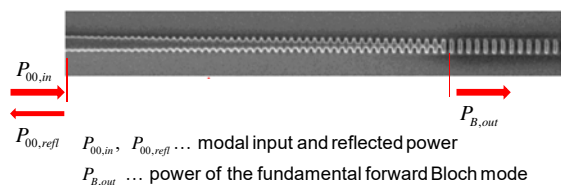
"Bridged" section $\sim 3.38 \mu\text{m}$, 15 "periods", "unbridged" section $\sim 9.13 \mu\text{m}$, 27 "periods"

Version 4 (L/8)

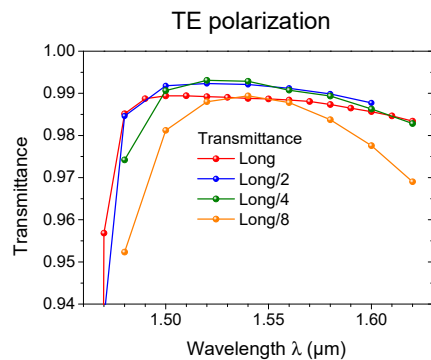
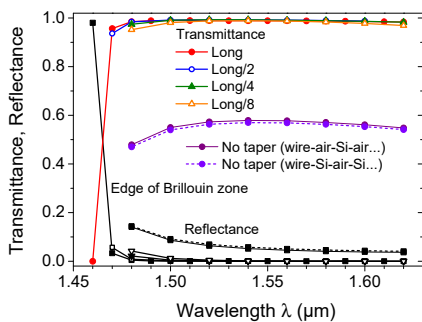
Similar (linearly tapered) but eight-times shorter: total length $\sim 6.25 \mu\text{m}$

"Bridged" section $\sim 1.69 \mu\text{m}$, 7 "periods", "unbridged" section $\sim 4.6 \mu\text{m}$, 13 "periods"

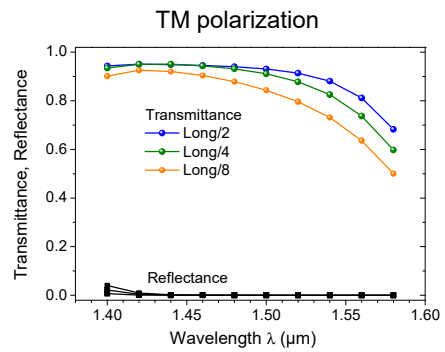
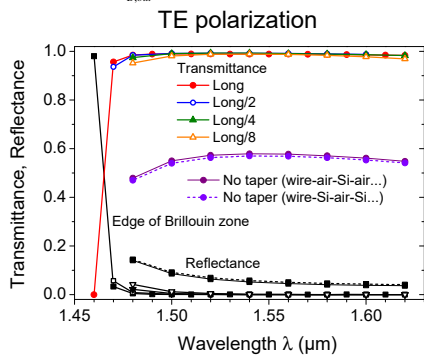
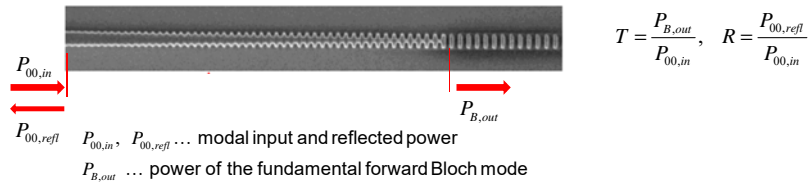
TRANSMITTANCE AND REFLECTANCE OF THE NANOWIRE TO SWGW COUPLER



$$T = \frac{P_{B,out}}{P_{00,in}}, \quad R = \frac{P_{00,refl}}{P_{00,in}}$$

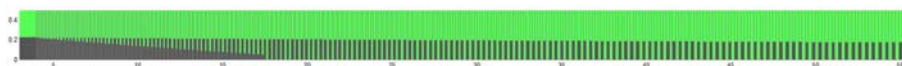


TRANSMITTANCE AND REFLECTANCE OF THE NANOWIRE TO SWGW COUPLER

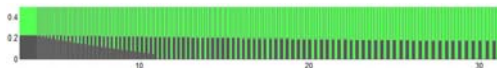


COUPLERS OF DIFFERENT LENGTHS

Version 1 (L) vertical view; only upper half is shown because of structure symmetry



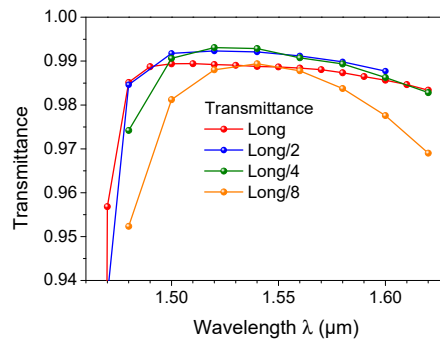
Version 2 (L/2)



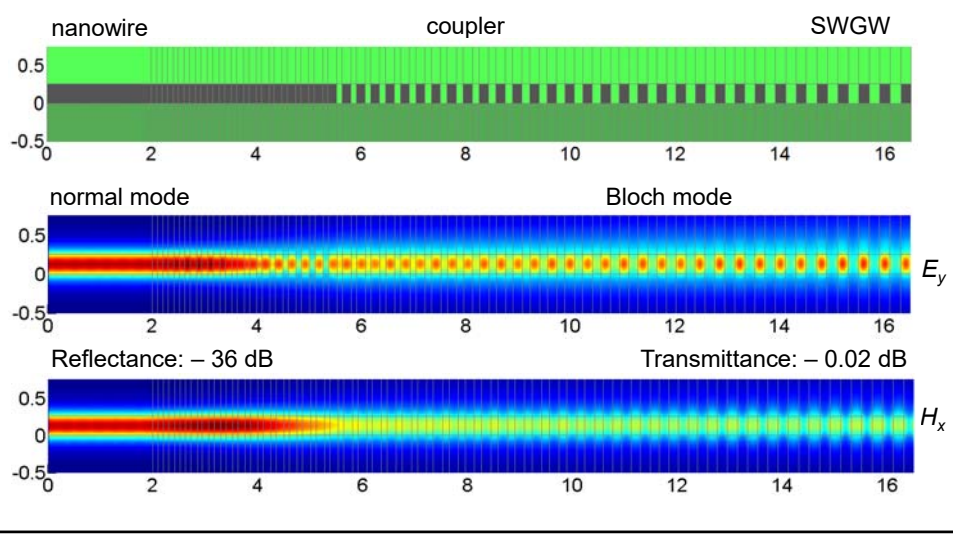
Version 3 (L/4)



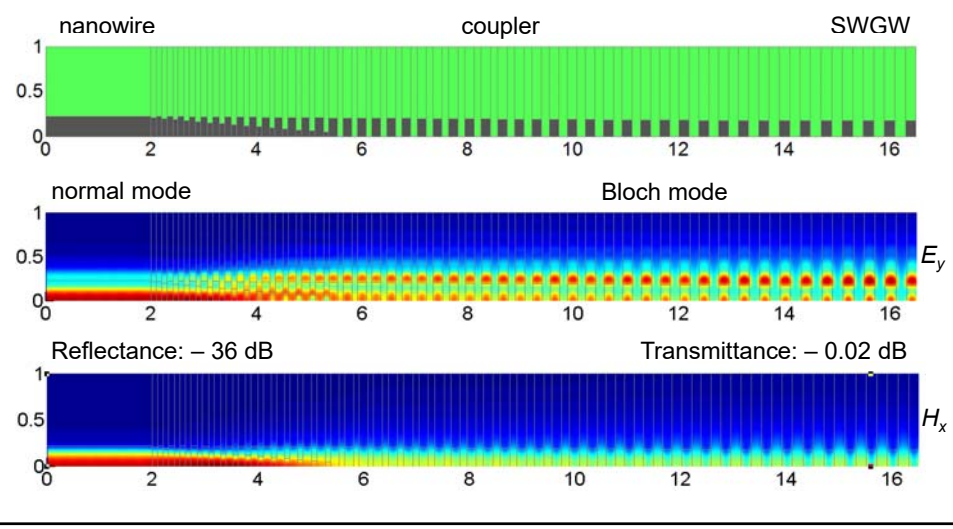
Version 4 (L/8)



TE₀₀ MODE FIELD DISTRIBUTION IN THE L/4 COUPLER: VERTICAL PLANE

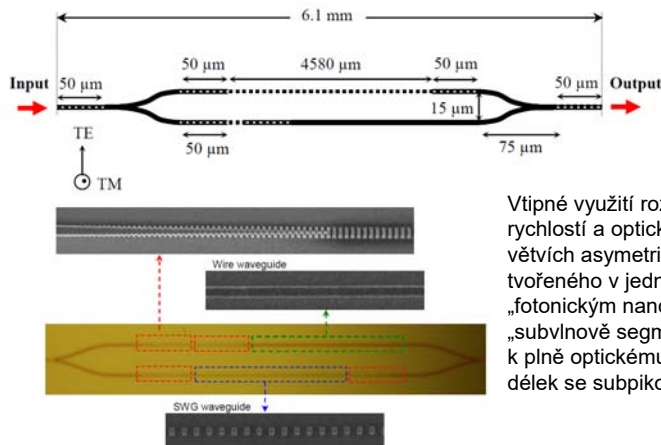


TE₀₀ MODE FIELD DISTRIBUTION IN THE L/4 COUPLER: HORIZONTAL PLANE (upper half)



Aplikace subvlnových segmentovaných vlnodů na optický konvertor vlnových délek

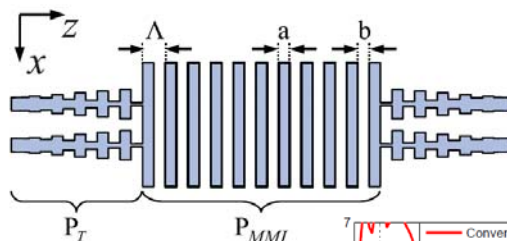
I. Glesk, P. J. Bock, P. Cheben *et al.*, Optics Express, 19 (15), 14031 (2011).



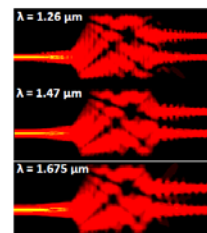
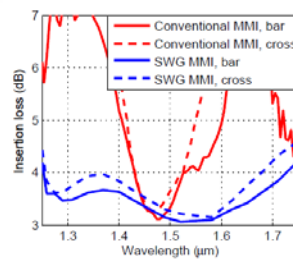
Vtipné využití rozdílu fázových a grupových rychlostí a optické lokalizace v jednotlivých větvích asymetrického MZ interferometru tvořeného v jedné větvi homogenním „fotonickým nanodrátem“ a ve druhé větvi „subvlnově segmentovaným“ vlnovodem k plně optickému spínání a konverzi vlnových délek se subpikosekundovou rychlostí

Aplikace subvlnových segmentovaných vlnodů na vazební člen s mnohovlnovou interferencí

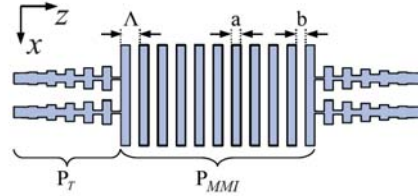
P. Cheben *et al.*, Wavelength-Independent Multimode Interference Coupler, Opt. Express 2012
NRC, Ottawa, Canada, and University of Malaga, Spain



Optimalizace parametrů umožňuje širokopásmové použití



BROADBAND SWGW MMI COUPLER

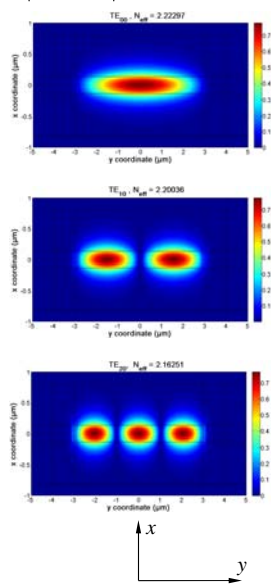


1. Optimization of MMI section for broadband operation
2. Check of imaging properties of the MMI section
3. Verification of taper function
4. Analysis of possible mutual coupling between tapers
5. Field distribution and scattering matrix of the complete coupler

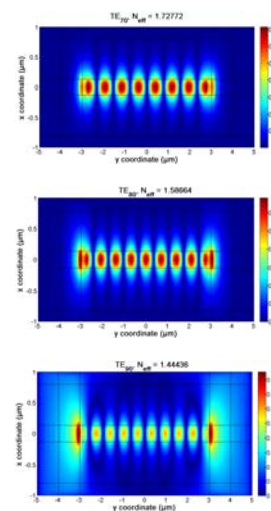
A. Maese-Novo, R. Halir, S. Romero-García, D. Pérez-Galacho, L. Zavargo-Peche, A. Ortega-Moñux, I. Molina-Fernández, J. G.Wangüemert-Pérez, and P. Cheben, *Opt. Express* vol 21, 7033-7040 (2013)

BLOCH MODES IN THE SWG MULTIMODE REGION

$|E_y(x, y)|$, $\lambda = 1.55 \mu\text{m}$



$\Lambda = 180 \text{ nm}$

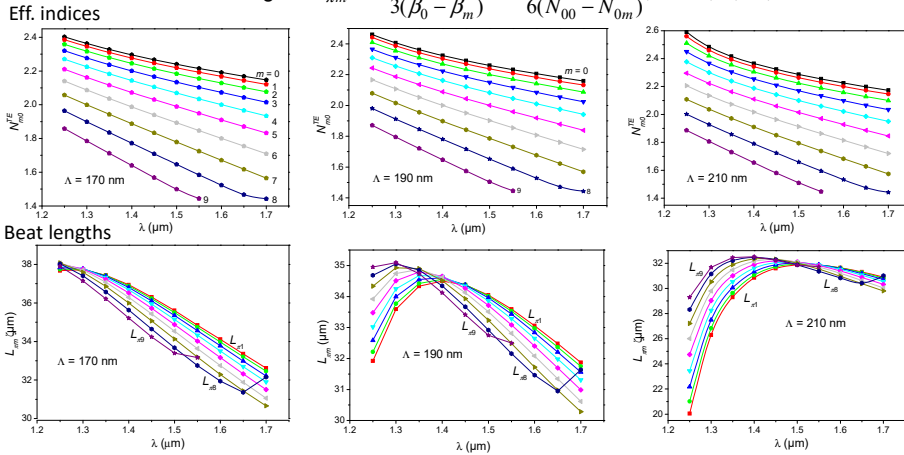


TE_{90} mode is weakly guided and for $\lambda > 1.55 \mu\text{m}$ is cut-off

OPTIMIZATION OF MMI SECTION FOR BROADBAND OPERATION

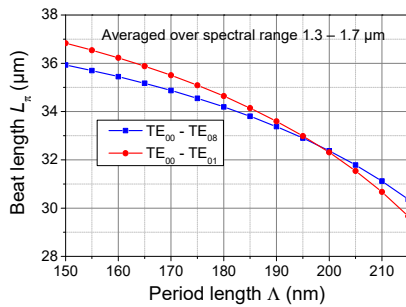
Minimize wavelength dependence of the beat length between several lowest-order lateral Bloch modes by optimization of period length; MMI section width = 6 μm

$$\text{"ideal" beat length: } L_{\pi m} = \frac{[(m+1)^2 - 1]\pi}{3(\beta_0 - \beta_m)} = \frac{m(m+2)}{6(N_{00} - N_{0m})}, \quad m = 1, 2, \dots, 8$$

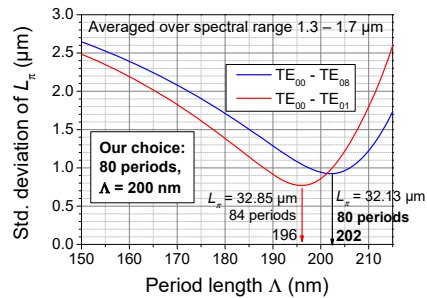


OPTIMIZATION OF THE MMI SECTION FOR 1.3 – 1.7 μm WAVELENGTH RANGE

Average beat lengths



Standard deviations of the beat lengths



Averaging over wavelengths and modes:

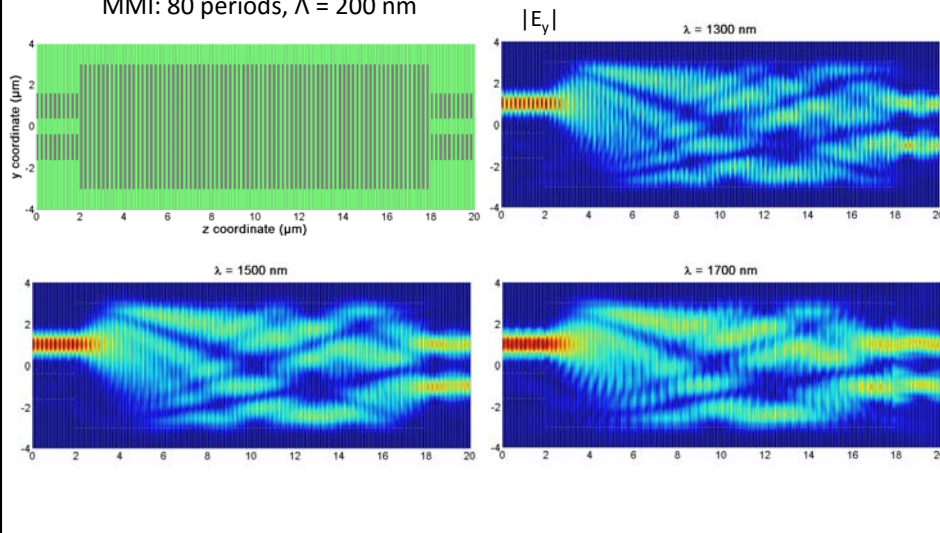
$$\Lambda_{opt}^{0-1} = 196 \text{ nm}, \quad L_{\pi}^{0-1} = 32.85 \text{ } \mu\text{m}, \quad NoP^{0-1} \doteq L_{\pi}^{0-1} / (2\Lambda_{opt}^{0-1}) = 84 \text{ periods},$$

$$\Lambda_{opt}^{0-8} = 202 \text{ nm}, \quad L_{\pi}^{0-8} = 32.13 \text{ } \mu\text{m}, \quad NoP^{0-8} \doteq L_{\pi}^{0-8} / (2\Lambda_{opt}^{0-8}) = 80 \text{ periods}.$$

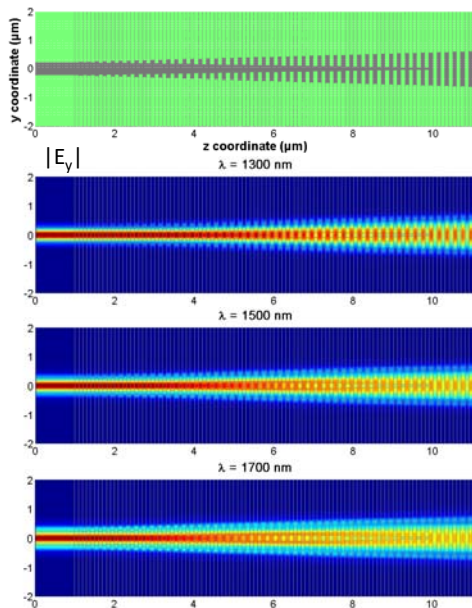
IMAGING PROPERTIES OF THE SWG MMI SECTION

Excitation of the SWG MMI section with SWG "ports"
by the superposition of symmetric and antisymmetric Bloch modes

MMI: 80 periods, $\Lambda = 200$ nm



PROPERTIES OF INPUT AND OUTPUT COUPLERS



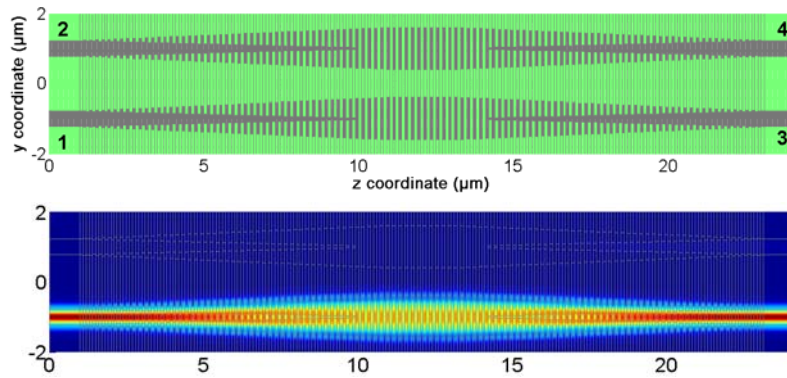
Estimated SWG period $\Lambda = 200$ nm

Conversion from photonic wire
into Bloch mode of the SWG output:

Very high conversion efficiency
difficult to reliably calculate
(loss ≤ 0.01 dB),
very small return loss –
reflected power ≤ -45 dB
for all wavelengths
1.3 μm , 1.5 μm , and 1.7 μm .

Shorter taper could probably
work well, too.

CHECK OF MUTUAL COUPLING IN THE TAPERS

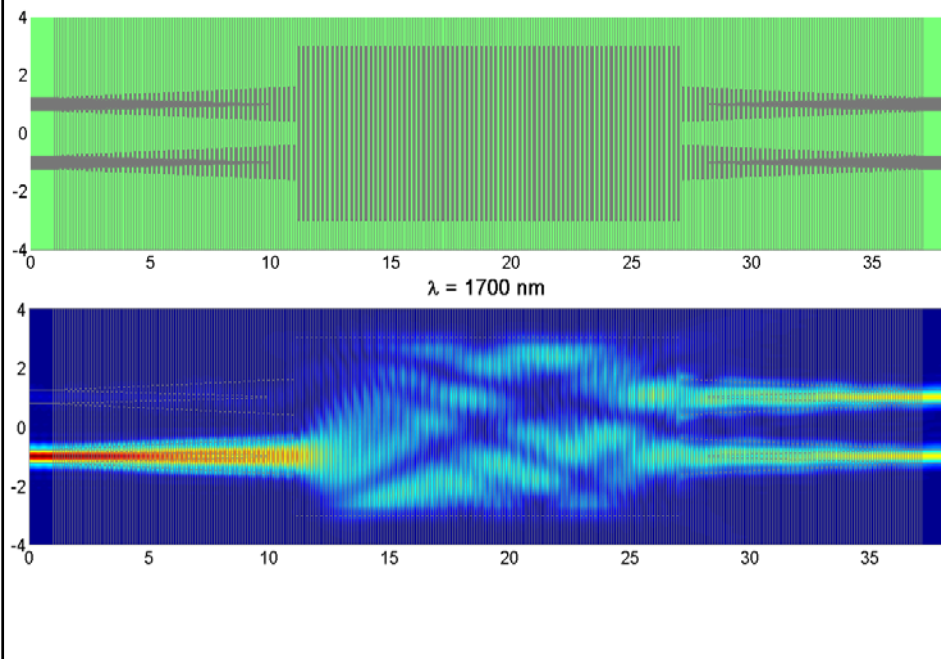


Calculated scattering parameters:

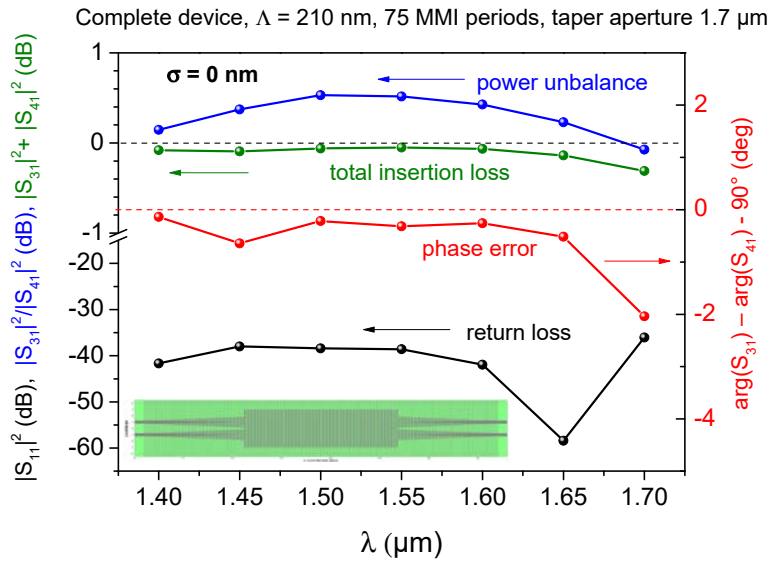
λ (μm)	$ S_{11} ^2$	$ S_{31} ^2$	$ S_{41} ^2$	Loss
1.70	2.304×10^{-5}	0.995	4.963×10^{-3}	-1.561×10^{-5}
1.50	2.804×10^{-5}	0.993	6.991×10^{-3}	-2.611×10^{-4}
1.30	4.149×10^{-5}	0.988	1.260×10^{-2}	-3.966×10^{-4}

Mutual coupling in tapers is unimportant

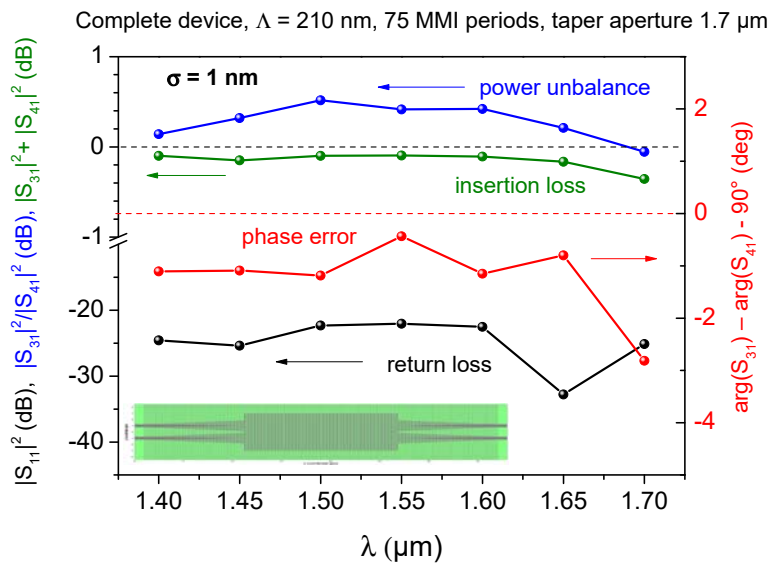
FIELD DISTRIBUTION IN THE SWG MMI COUPLER



S-PARAMETERS OF THE COMPLETE MMI DEVICE

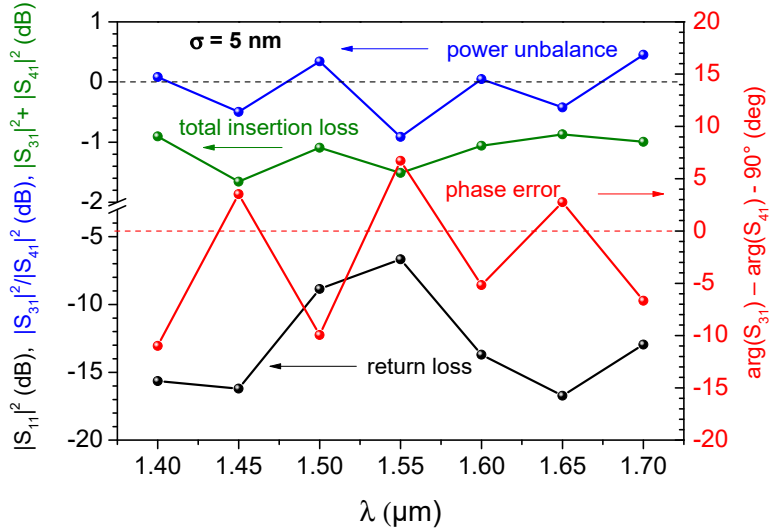


INFLUENCE OF RANDOM FLUCTUATIONS

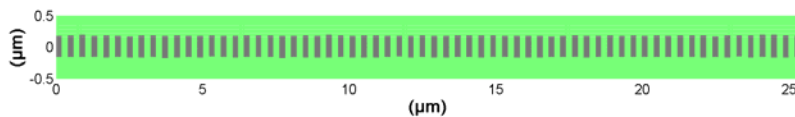


INFLUENCE OF RANDOM FLUCTUATIONS

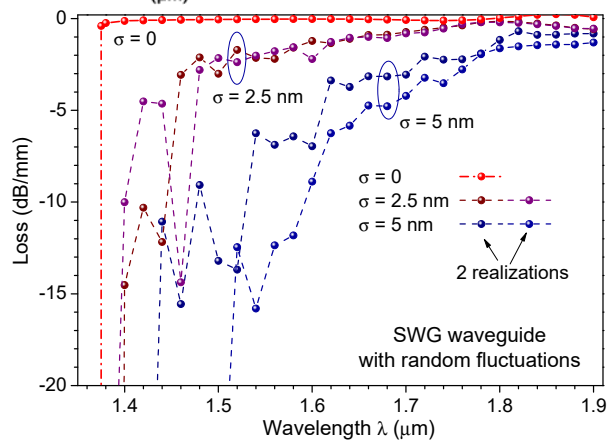
Complete device, $\Lambda = 210$ nm, 75 MMI periods, taper aperture $1.7 \mu\text{m}$



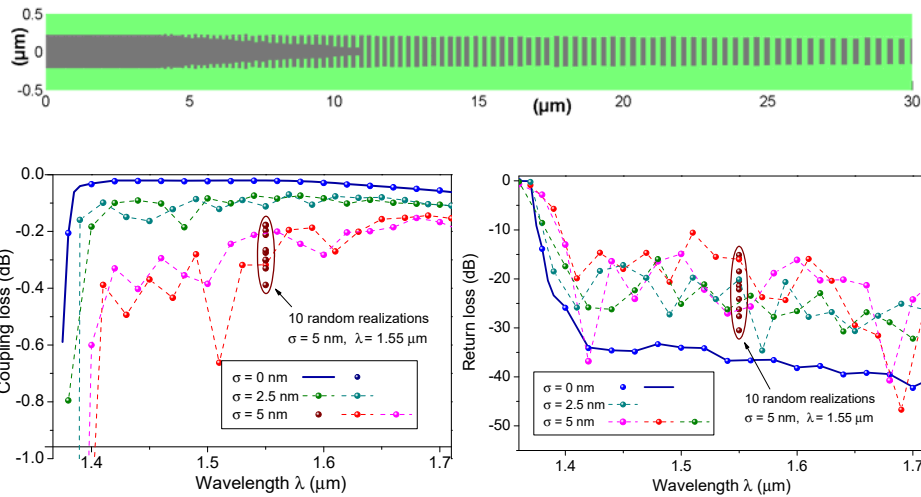
INFLUENCE OF RANDOM FLUCTUATIONS ON SWGW PERFORMANCE



Positions and dimensions of Si segments fluctuate with normal distribution and standard deviation σ

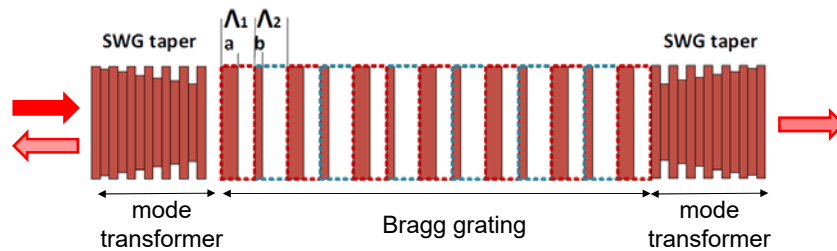


INFLUENCE OF RANDOM FLUCTUATIONS ON SWGW COUPLER PERFORMANCE

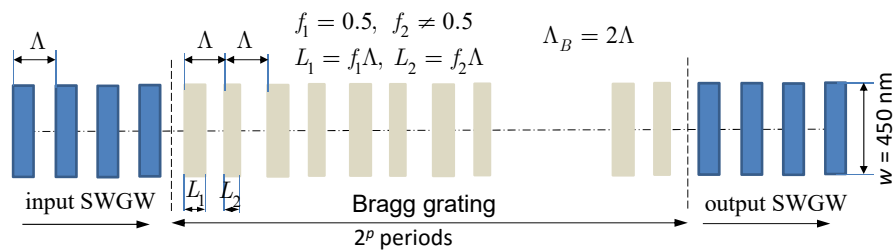


Simulations of Bragg gratings

2.5-D FDTD: excitation with the mode of a Si nanowire

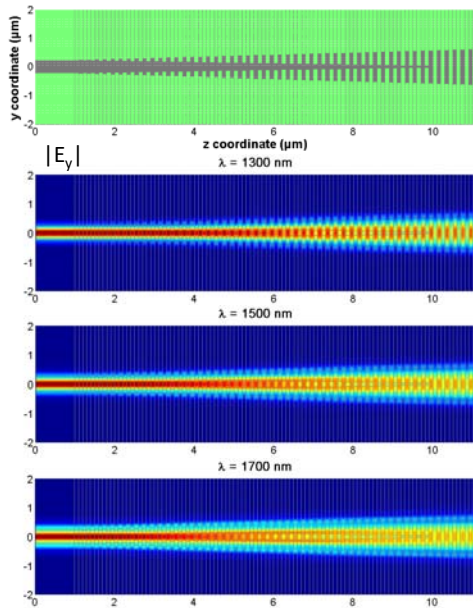


Fourier Modal Method(s): excitation with a Bloch mode of a SWG waveguide



39

I/O mode transformers are supposed to perform perfectly



Results of previous simulations of similar structures:

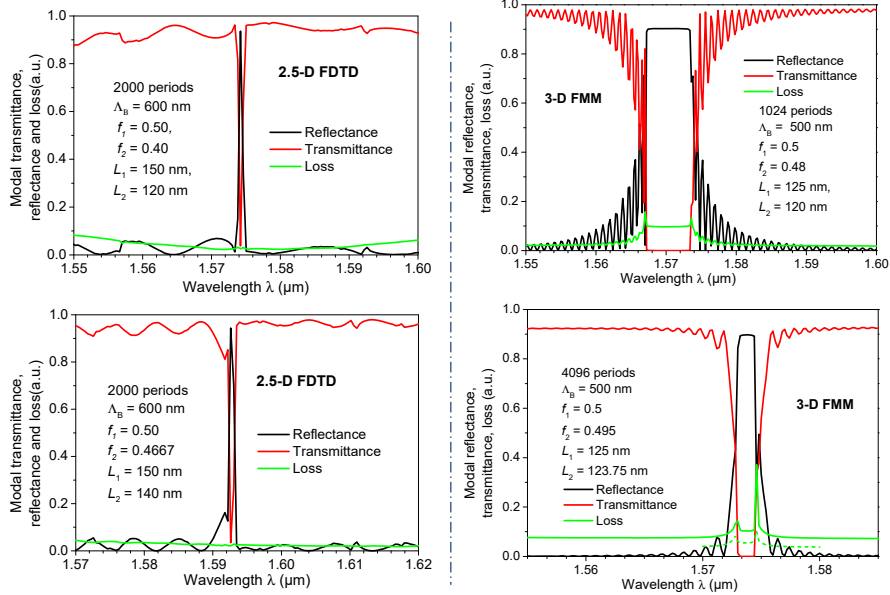
SWG period $\Lambda = 200$ nm
Conversion from photonic wire into Bloch mode of the SWG output:

Very high conversion efficiency
difficult to reliably calculate
(loss as low as 0.01 dB);
very small return loss:
reflected power ≤ -45 dB
for wavelengths
1.3 μm , 1.5 μm , and 1.7 μm .

Shorter couplers could probably perform well enough, too.

40

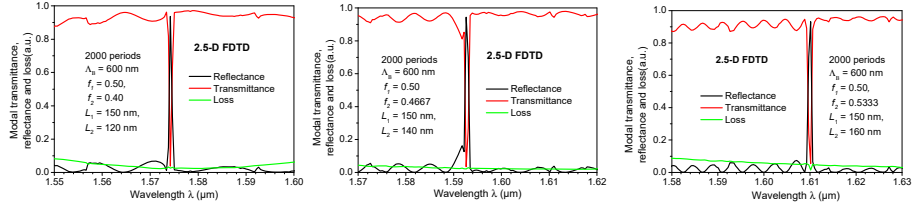
Comparison of calculated spectral characteristics



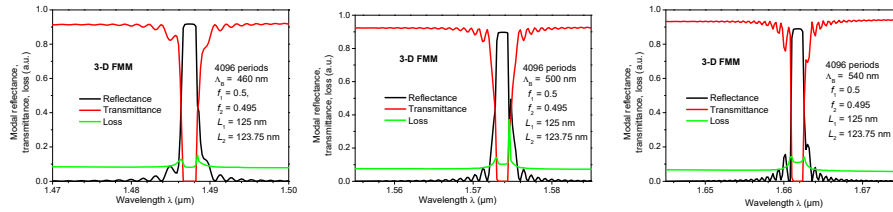
41

“Spectral tuning” of SWG waveguide Bragg gratings

2.5-D FDTD: Change of the duty cycle of the Bragg grating



3-D FMM: Change of the period of the Bragg grating



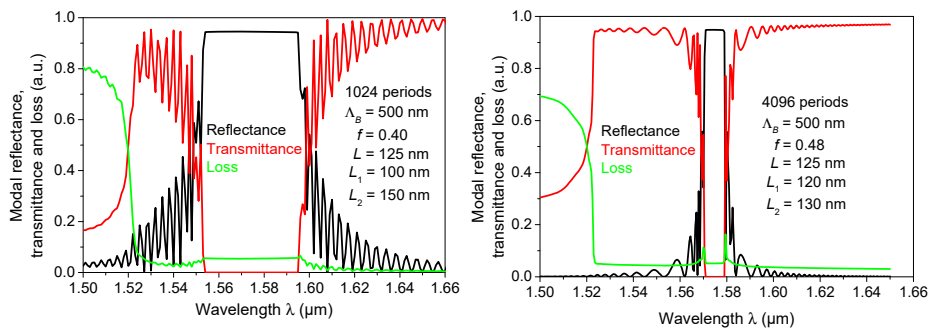
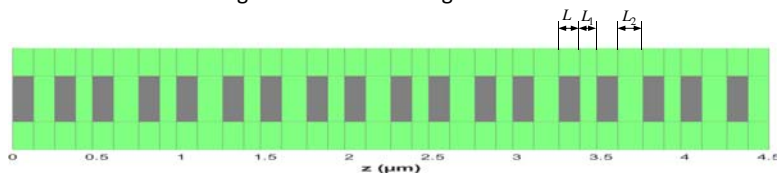
Extremely small modulation of the duty cycle is required for narrow-band operation!

42

Another possible configuration of SWGW Bragg grating

realizable using single-step lithography

Position modulation of Si segments in SWG waveguide



43